

### Nonlocal conductivity in Bi<sub>2</sub>Sr<sub>2</sub>CaCu<sub>2</sub>O<sub>8+δ</sub> crystals

C. D. Keener, M. L. Trawick, S. M. Ammirata, S. E. Hebboul, and J. C. Garland

Department of Physics, Ohio State University, Columbus, Ohio 43210

(Received 7 August 1996)

Using an eight-terminal geometry, we have measured voltages in Bi<sub>2</sub>Sr<sub>2</sub>CaCu<sub>2</sub>O<sub>8+δ</sub> single crystals with current injected both parallel and perpendicular to the crystallographic *c* axis and with magnetic fields  $H \leq 3$  kOe,  $\mathbf{H} \parallel c$  axis. In a range of fields and temperatures for which the conductivity is Ohmic, our results disagree with a model that assumes classical electrodynamics. We believe that interlayer vortex coupling is responsible for nonlocal conductivity in this regime. [S0163-1829(97)50902-7]

Although the motion of continuous vortex lines in high-temperature superconducting crystals is believed to induce nonlocal conductivity over distances of several  $\mu\text{m}$ ,<sup>1-3</sup> the existence of such continuous lines in the vortex liquid phase has been a matter of dispute. Based on transport data that could not be explained by classical electrodynamics, Safar *et al.*<sup>1</sup> have concluded that the conductivity of YBa<sub>2</sub>Cu<sub>3</sub>O<sub>7+δ</sub> (YBCO) above the vortex lattice melting temperature is nonlocal. Eltsev and Rapp<sup>4</sup> have challenged their interpretation, and other investigators also remain doubtful.<sup>5</sup> In contrast to their findings in YBCO, Safar *et al.*<sup>6</sup> found no evidence for nonlocal conductivity in Bi<sub>2</sub>Sr<sub>2</sub>CaCu<sub>2</sub>O<sub>8+δ</sub> (BSCCO) for applied magnetic fields  $H \geq 5$  kOe.

Nonlocal conductivity is a signature of interlayer vortex coupling. In the presence of a magnetic field, a driving current concentrated near one surface of a crystal will induce vortex motion at the opposite surface only if some vortices are coupled over the entire sample thickness. This vortex motion then produces dissipation which manifests itself as an electric field or a voltage. Huse and Majumdar<sup>2</sup> express the nonlocal resistivity generally using the electric field  $\mathbf{E}$  at point  $\mathbf{r}$ ,

$$E_\alpha(\mathbf{r}) = \int d\mathbf{r}' \rho_{\alpha\beta}^{(nl)}(\mathbf{r}-\mathbf{r}') j_{\beta b}(\mathbf{r}'),$$

where  $\rho_{\alpha\beta}^{(nl)}(\mathbf{r})$  is the nonlocal resistivity tensor and  $\mathbf{j}$  is the current density; local conductivity is recovered in the special case where  $\rho_{\alpha\beta}^{(nl)}(\mathbf{r}-\mathbf{r}') = \rho_{\alpha\beta}(\mathbf{r}) \delta(\mathbf{r}-\mathbf{r}')$ .

In this paper we present evidence for nonlocal conductivity in the vortex liquid phase of BSCCO single crystals. In recently reported transport measurements using an eight-terminal sample geometry, we have found that within a small region below the equilibrium melting temperature a transport current drives vortices into a nonequilibrium line liquid state delimited by distinct vortex lattice melting and line decoupling transitions at temperatures  $T_m$  and  $T_D$ , respectively.<sup>7</sup> In this work we will explore nonlocal conductivity above the decoupling temperature  $T_D$ , where our measurements suggested that the rapidly decaying interlayer vortex coupling is significant over a range of a few kelvin. We have used the method of Safar *et al.*<sup>1</sup> to calculate two independent values of the resistivity anisotropy  $\rho_c/\rho_{a,b} = \gamma^2$ , one from voltages

measured with current  $I$  injected along the *ab* plane ( $\gamma_{ab}^2$ ) and the other with  $I \parallel \hat{c}$  ( $\gamma_c^2$ ). Safar's method, which is based in part on the analysis of Montgomery,<sup>8</sup> assumes local and Ohmic conductivity. For  $50 \text{ Oe} < H < 3 \text{ kOe}$  (lower fields than in Ref. 6),  $\gamma_{ab}^2$  and  $\gamma_c^2$  do not agree. This discrepancy between the two calculations of  $\gamma^2$  demonstrates a breakdown of the Montgomery model and thus (in a temperature range where transport behavior is Ohmic) a breakdown of the assumption of local conductivity.

BSCCO single-crystal samples whose lateral dimensions were typically  $1 \text{ mm} \times 0.5 \text{ mm}$ , with thicknesses of  $1-20 \mu\text{m}$ , were grown by a self-flux technique and cleaved to achieve optically smooth surfaces with the *c* axis normal to the sample surface.<sup>7</sup> Next, eight silver pads were photolithographically patterned onto the top and bottom surfaces of the crystals, as shown in Fig. 1. Pads on the two surfaces were in alignment with one another, and bottom pads extended beyond the edge of the crystals to facilitate wire bonding. Crystals were then annealed in O<sub>2</sub> at  $600^\circ\text{C}$  for two hours, and, finally,  $0.7 \text{ mil}$  gold wires were ultrasonically bonded to the pads. The results discussed here are for a  $1 \text{ mm} \times 0.3 \text{ mm} \times 1.1 \mu\text{m}$  crystal (thickness measured in a JEOL 5400 scanning electron microscope). The center-to-center distances between contacts were measured in an optical microscope to be

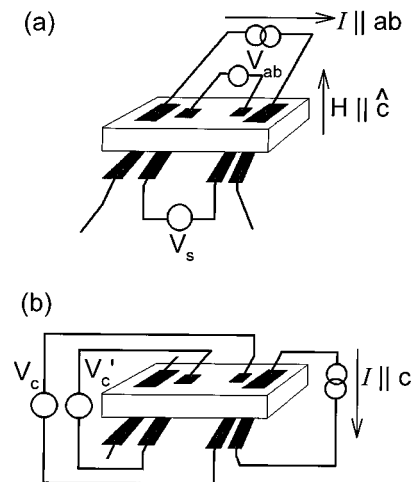


FIG. 1. The sample and electrode configuration for (a) in-plane current and (b)  $I \parallel \hat{c}$ .

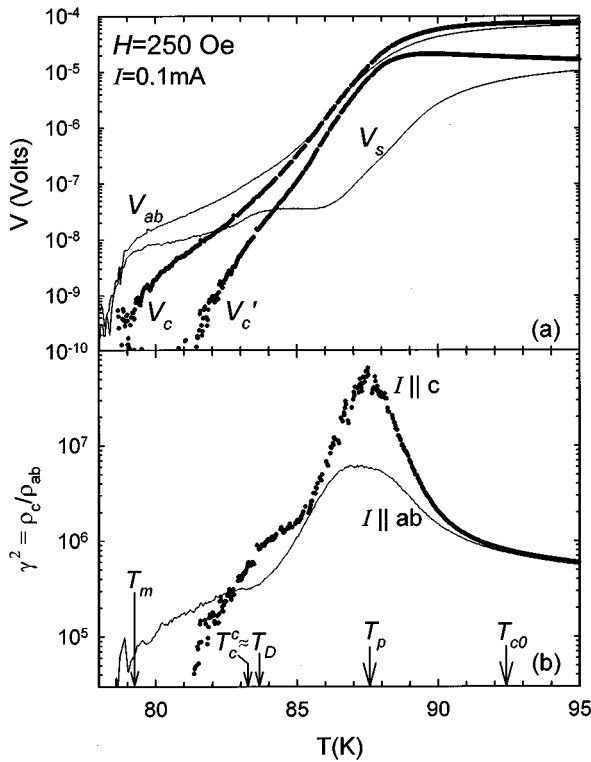


FIG. 2. (a) Voltages  $V_{ab}$ ,  $V_s$  (lines),  $V_c$ , and  $V'_c$  (symbols) as functions of temperature for  $I=0.1$  mA, and  $H=250$  Oe. (b) Apparent anisotropy  $\gamma_{ab}^2$  (line) and  $\gamma_c^2$  (symbols) calculated using the Montgomery model from the data of (a). Temperatures defined in the text are labeled in the figure as  $T_{c0}$ ,  $T_p$ ,  $T_c^c$ ,  $T_D$ , and  $T_m$ .

0.28 mm between voltage pads and 0.10 mm between adjacent voltage and current pads.

Figure 1 shows the sample geometry and electrode configurations for  $I \parallel \hat{ab}$  and  $I \parallel \hat{c}$ . In our notation,  $V_{ab}$  is the voltage measured on the surface into which current  $I \parallel \hat{ab}$  is injected, and  $V_s$  is the voltage measured on the opposing surface. As an indicator of consistency,  $V_{ab}$  and  $V_s$  were found to be independent of the surface into which current was injected (except for  $\leq 6\%$  difference at the peak in  $V_s(T)$  for  $H \leq 50$  Oe). Two voltages  $V_c$  and  $V'_c$  were measured with  $I$  injected parallel to  $\hat{c}$ , as shown in the figure.

Figure 2(a) shows the above-described sample voltages as a function of temperature  $T$ , measured in a magnetic field of 250 Oe and a current of 0.1 mA. We applied the modified Montgomery analysis of Safar *et al.*<sup>1</sup> to calculate  $\gamma_{ab}^2(T)$  and  $\gamma_c^2(T)$ , shown in Fig. 2(b). At 95 K in the normal state, the two calculations of  $\gamma^2$  agree remarkably well; the difference of 9% can be accounted for by the uncertainty in sample dimensions. Notably, however, at  $T_{c0}=92.4$  K, the zero-field onset of the  $c$ -axis resistivity transition,  $\gamma_{ab}^2(T)$  and  $\gamma_c^2(T)$  diverge from one other. The discrepancy between them reaches a maximum at the temperature  $T_p$  of the peak in  $\gamma_c^2(T)$ , 87.6 K, where  $\gamma_c^2(T_p)/\gamma_{ab}^2(T_p)=9.7$ .

The temperature  $T_p$  is well within the range for which  $c$ -axis conductivity is Ohmic. We define  $T_c^c$  to be the temperature below which  $c$ -axis  $I$ - $V$  characteristics are nonlinear, as it is defined by Wan *et al.*<sup>9</sup> In this experiment, we determined  $T_c^c$  from the separation of  $V'_c/I$  vs  $T$  curves mea-

sured using different applied currents. Estimating  $T_c^c$  by extrapolating  $\rho_c(T)$  in its Ohmic regime ( $T > T_c^c$ ) to zero<sup>10</sup> does not affect our result. In both high<sup>10</sup> and low<sup>9</sup>  $H$ ,  $T_c^c(H)$  is higher than the temperature at which in-plane resistivity  $\rho_{ab} \rightarrow 0$ . In this experiment  $T_c^c$  (250 Oe) =  $(83.3 \pm 0.2)$  K.

Note that only nonlocal conductivity can account for a disagreement from the Montgomery model for  $T > T_c^c$ , where  $I$ - $V$  characteristics are linear (Ohmic). Thus the large discrepancy from the Montgomery model for  $T_p \leq T \leq 90$  K arises from significant nonlocal conductivity over a distance of  $\sim 1$   $\mu\text{m}$ . Note also that we expect significant interlayer coupling just above the decoupling transition temperature  $T_D$ .<sup>7</sup> From the ratio  $V_s/V_{ab}$  as a function of temperature,  $T_D$  was determined to be 83.7 K,<sup>7</sup> so that  $T_c^c \approx T_D$  [in higher fields also,  $T_c^c(H) \approx T_D(H)$  (Ref. 10)]. As we expected, since  $T_p$  is not very far above  $T_D$  and is well below the normal-state temperature  $T_{c0}$ , interlayer coupling demonstrated by nonlocal conductivity remains strong at  $T_p$ . This result confirms that conductivity in BSCCO may still be nonlocal when  $V_s < V_{ab}$ , just as conductivity was nonlocal above  $T_m$  in YBCO.<sup>1</sup> In other words, some correlated vortex motion may be present without all vortices forming perfectly correlated lines, and a detailed analysis of the data is necessary in order to detect finite-range nonlocal effects.

This observed nonlocal conductivity seems to be an effect intrinsic to BSCCO and is probably not the result of pinning at extended defects such as twinning boundaries, which have been shown to enhance interlayer coupling in YBCO.<sup>11</sup> If a significant number of strongly pinning defects were present in our samples, the first-order melting transition that is evident in Fig. 2 from the sharp drop in  $V_{ab}(T)$  at  $T_m$  probably would have been suppressed.<sup>1,11,12</sup> The main differences between this work and previous studies in BSCCO<sup>6,13</sup> are the lower range of fields being explored ( $H \leq 3$  kOe vs  $H \geq 5$  kOe) and the shorter distance over which nonlocal effects are being probed (sample thickness  $\sim 1$   $\mu\text{m}$  vs  $\geq 10$   $\mu\text{m}$ ).

For  $T \leq T_c^c$ , we believe that the nonlinear  $c$ -axis  $I$ - $V$  characteristics (which cause a breakdown of the Montgomery analysis) arise from the intrinsic Josephson effect.<sup>14</sup> In the range 80–85 K for  $H=250$  Oe,  $V_c - 0.2 V_{ab} = 2.5 V'_c$ , suggesting that most of the long low-temperature tail in  $V_c(T < T_c^c)$  suggesting that most of the long low-temperature tail in  $V_c(T < T_c^c)$  comes from a voltage drop where current is flowing across the  $ab$  plane. As a further indication of in-plane currents, in somewhat higher magnetic fields (e.g., 350 Oe), the sharp drop at  $T_m$  in  $V_{ab}(T)$  is actually apparent in  $V_c(T)$ . Because of the high anisotropy of BSCCO and the intrinsic Josephson junctions that form below  $T_c^c$ ,<sup>14</sup> part of the current that is injected  $\parallel \hat{c}$  may flow from one current contact, beyond the voltage contacts, and then back to the current contact on the opposite surface, so that  $\rho_{ab}$  contributes significantly to  $V'_c$  and especially to  $V_c$ , which is measured nearer to the current leads. The intrinsic Josephson effect may also increase the effective anisotropy below  $T_c^c$  for  $I \parallel \hat{ab}$ , because current injected parallel to the planes tends to be confined near the surface rather than tunnel through the layers.

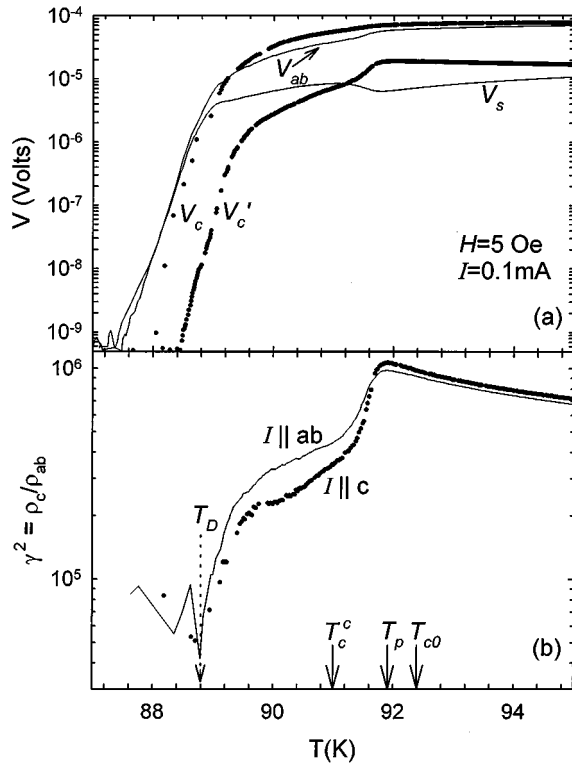


FIG. 3. (a) Voltages  $V_{ab}$ ,  $V_s$  (lines),  $V_c$ , and  $V'_c$  (symbols) as functions of temperature for  $I=0.1$  mA and  $H=5$  Oe. (b) Apparent anisotropy  $\gamma_{ab}^2$  (line) and  $\gamma_c^2$  (symbols) calculated from the data of (a). Temperatures  $T_{c0}$ ,  $T_p$ ,  $T_c^c$ , and  $T_D$  are shown.

In Fig. 3(a) the voltages  $V_{ab}$ ,  $V_s$ ,  $V_c$ , and  $V'_c$  are plotted as functions of temperature for a field of 5 Oe and a current of 0.1 mA; Fig. 3(b) shows  $\gamma_{ab}^2(T)$  and  $\gamma_c^2(T)$ . (Data are plotted for  $H=5$  Oe rather than for  $H=0$ , so that  $T_D$  is defined.) In this low applied field,  $T_c^c \approx 91$  K, and  $T_D = 88.8$  K, so that  $T_p$  ( $=91.9$  K) is well defined above  $T_D$  and near  $T_{c0}$ , where interlayer coupling should be small. Note that the discrepancy between  $\gamma_{ab}^2(T)$  and  $\gamma_c^2(T)$  is small over the entire temperature range. Since the Montgomery model is applicable only above  $T_c^c$ , our results here indicate local conductivity only for  $T > T_c^c$ . In these low fields dissipation is dominated by the motion of thermally excited vortices,<sup>9</sup> which we have previously shown are decoupled above  $T_c^c$ , in agreement with this result. Pierson<sup>15</sup> and Friesen<sup>16</sup> have predicted a diverging interlayer coupling correlation length near the zero resistance temperature in zero field. In accord with

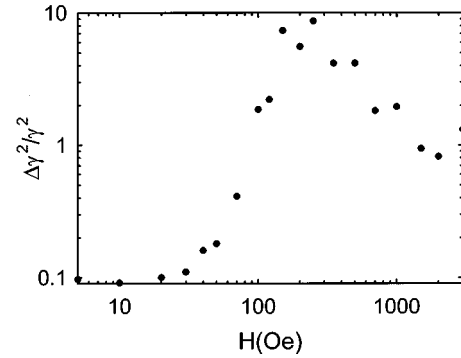


FIG. 4. Discrepancy  $\Delta \gamma^2 / \gamma^2$  of the data from the Montgomery model [calculated at the temperature of the peak in  $\gamma_c^2(T)$ ] as a function of applied magnetic field.

their theoretical work, we find that  $V_s$  approaches  $V_{ab}$  below  $T_D$ , suggesting that interlayer vortex coupling is strong near  $T_D$ .

In order to summarize our results for all  $H \leq 3$  kOe, we define the discrepancy between  $\gamma_c^2$  and  $\gamma_{ab}^2$  at  $T_p$ :

$$\frac{\Delta \gamma^2}{\gamma^2} = \frac{\gamma_c^2(T_p) - \gamma_{ab}^2(T_p)}{\gamma_{ab}^2(T_p)}.$$

Figure 4 shows  $\Delta \gamma^2 / \gamma^2$  as a function of  $H$ . This discrepancy signifies the strength of interlayer vortex coupling which gives rise to nonlocal conductivity. As we mentioned above, in low fields  $H \leq 50$  Oe,  $\Delta \gamma^2 / \gamma^2$  is small because  $T_p$  is near  $T_{c0}$ . In the regime  $T_D < T < T_c^c$ , where a broad peak appears in  $V_s(T)$ , thermally excited vortices are the dominant source of dissipation. For  $H > 50$  Oe, where thermally excited vortices are less important, interlayer coupling does affect transport behavior near  $T_p$ , which is farther from  $T_{c0}$ . As  $H$  increases above 250 Oe, however, in-plane interactions among vortex lines tend to decouple the layers. An analogous process of interlayer decoupling in high fields occurs within the vortex solid,<sup>17,18</sup> where there may be a second-order transition between a low-field vortex lattice and a high-field glasslike phase.<sup>18</sup> In the vortex liquid, however, this high-field decoupling appears to be a gradual process, since the amount of disagreement from local conductivity shown in Fig. 4 does not exhibit any discontinuity in fields up to 3 kOe.

This work was supported by the Midwest Superconductivity Consortium through DOE Contract No. DE-FG02-90ER45427 and by NSF Grant No. DMR 95-01272.

<sup>1</sup>H. Safar *et al.*, Phys. Rev. Lett. **72**, 1272 (1994).

<sup>2</sup>D. A. Huse and S. N. Majumdar, Phys. Rev. Lett. **71**, 2473 (1993).

<sup>3</sup>D. López *et al.*, Phys. Rev. B **50**, 9684 (1994); F. de la Cruz, D. López, and G. Nieva, Philos. Mag. B **70**, 773 (1994); D. López *et al.*, Phys. Rev. Lett. **76**, 4034 (1996).

<sup>4</sup>Yu. Eltsev and Ö. Rapp, Phys. Rev. Lett. **75**, 2446 (1995).

<sup>5</sup>E. H. Brandt, Rep. Prog. Phys. **58**, 1465 (1995), see especially pp. 1508–1511.

<sup>6</sup>H. Safar *et al.*, Phys. Rev. B **46**, 14 238 (1992).

<sup>7</sup>C. D. Keener, M. L. Trawick, S. M. Ammirata, S. E. Hebboul, and J. C. Garland (unpublished).

<sup>8</sup>H. C. Montgomery, J. Appl. Phys. **42**, 2971 (1971).

<sup>9</sup>Y. M. Wan *et al.*, Phys. Rev. Lett. **71**, 157 (1993); **72**, 3867 (1994); **74**, 5286(E) (1995).

<sup>10</sup>M. C. Hellerqvist *et al.*, Physica C **230**, 170 (1994); J. H. Cho *et al.*, Phys. Rev. B **50**, 6493 (1994).

<sup>11</sup>D. López, *et al.* Phys. Rev. B **53**, R8895 (1996).

- <sup>12</sup>J. A. Fendrich *et al.*, Phys. Rev. Lett. **74**, 1210 (1995).  
<sup>13</sup>R. Busch *et al.*, Phys. Rev. Lett. **69**, 522 (1992).  
<sup>14</sup>R. Kleiner, F. Steinmeyer, G. Kunkel, and P. Müller, Phys. Rev. Lett. **68**, 2394 (1992); R. Kleiner and P. Müller, Phys. Rev. B **49**, 1327 (1994),  
<sup>15</sup>S. W. Pierson, Phys. Rev. Lett. **75**, 4674 (1995).  
<sup>16</sup>M. Friesen, Phys. Rev. B **51**, 632 (1995); **51**, 12 786 (1995).  
<sup>17</sup>S. L. Lee *et al.*, Phys. Rev. Lett. **71**, 3862 (1993); **75**, 922 (1995).  
<sup>18</sup>B. Khaykovich *et al.*, Phys. Rev. Lett. **76**, 2555 (1996).